Article

Measurement of Group Delay Ripples of Chirped Fiber Bragg Gratings for CPA Lasers, and Their Effect on Performance

[François Ouellette](#) [*] and Hui Wang

Article

Measurement of Group Delay Ripples of Chirped Fiber Bragg Gratings for CPA Lasers, and their Effect on Performance

François Ouellette [1,*,†] and **Hui Wang** [2,†]

1   School of Electronic Information and Electrical Enginering, Chengdu University, Chengdu 130012, China;
    fouellette58@yahoo.ca
2   Ultron Photonics, Hangzhou, China
*   Correspondence: fouellette58@yahoo.ca
†   These authors contributed equally to this work.

Abstract: The group delay response of chirped fiber Bragg gratings (CFBG) written in polarization-maintaining fiber can be measured using the beat spectrum of the reflections from the two polarization axis, with a resolution and reproducibility better than 50 fs. The method is theoretically described, and we analyze the effect of group delay ripples (GDR) on the performance of a stretcher-compressor pair used in chirped pulse amplification systems. Ripples with a spectral period of the order of the pulse bandwidth are the most deleterious. Those are readily captured with our method, despite the limit on resolution due to the fiber polarization beat length. As a rule of thumb, the GDR should not exceed half the pulse duration. The reconstructed phase of the CFBG is also used to predict the pulse compression performance for a given device. Measurement of GDR as low as 161 fs is experimentally demonstrated.

Keywords: femtosecond laser; chirped pulse amplification; group delay ripples; chirped fiber Bragg grating; group delay measurement

---

1. Introduction

Chirped fiber Bragg gratings (CFBG) have proven to be invaluable components in fiber optic communication systems [1,2] as well as for chirped pulse amplification (CPA) laser systems[3–7], therefore accurate measurement of their group velocity dispersion (GVD), and especially their group delay ripples (GDR), is essential for assessing their performance [8–13].

The deleterious effects of GDR for CFBGs in optical communication links has been extensively studied, as well as methods to mitigate them [14–24]. Typically, however, CFBG bandwidths in such systems are around 0.5 nm, and the chirp is around 10 pm/mm. In such cases, GDR less than about 10 ps, or 20% of a bit length, are not causing significant impairment in terms of receiver sensitivity and bit-error-rate (BER) [17]. CPA laser systems have different characteristics and requirements. The CFBG bandwidth is typically much larger (10-20 nm), and the performance requirements are the duration of the recompressed pulse after amplification, as well as its quality, typically measured as the Strehl ratio. For pulses of a few 100's fs, it is intuitively apparent that GDR should be smaller than the pulse duration. That represents about a hundred times smaller GDR (100 fs vs 10 ps). An early study on the effect of GDR in a CPA system [19] concluded that GDR up to 10 ps were not affecting the quality or duration of the pulse, but that study only considered pulses in the picosecond domain. The conclusion was also based on the effect of GDR with a single spectral frequency, whereas GDR are typically more akin to noise. There has been so far no other detailed study on the performance requirements for sub-ps pulses, as well as accurate measurement of GDR.

Group velocity dispersion (GVD), and the associated GDR, are typically measured using a narrow band phase-modulated tunable light source [10,13,25]. The relative phase of the modulation sidebands is retrieved from the beat signal using a fast photodiode and a network analyzer, a method that involves expensive instrumentation. Other methods have been proposed and

demonstrated [9,12,26], but although some are presented as "simpler", they still involve complex and expensive equipment. Nevertheless, commercial instruments are available (e.g. Luna OVA5100 https://lunainc.com/product/ova-5100), that claim a resolution of 100 fs. Recently, we have presented a simple and inexpensive method to measure the GVD of CFBGs based on measuring the phase shift between the two orthogonal polarization modes of the optical fiber as a function of wavelength [27]. The method was originally used for dispersion compensators used in long distance fiber optic links [28], in which case the CFBG is typically written in circular core , non-polarization-maintaining (PM) fiber. For CPA systems, CFBGs are commonly made in PM fiber. In such cases, the polarization state goes through a large number of rotations along the CFBG, as opposed to a fraction of a cycle in non-PM fiber. However, we showed that our method could be adapted to reconstruct the phase from such a large number of cycles.

We show here that our method can accurately measure not only the various orders of GVD, but also fine group delay ripples down to better than 50 fs. We first analyze through simulations the origins and effect of such group delay ripples on the performance of the CFBG when used in a CPA stretcher/compressor system. The GDR are mostly due to spatial fluctuations in the CFBG period. Through the chirp of the grating, such fluctuations give rise to a spectral fluctuation of the phase, with higher spatial frequency fluctuations resulting in GDR with high spectral frequency. We show that, similar to what was described in Ref.[19], GDR with spectral periods of the order of the pulse bandwidth are the most deleterious, corresponding to fluctuations in the grating period on spatial scales of multiple millimeters. Although the resolution of our measurement method is limited by the beat length of the PM fiber, which is typically about 2.5 mm, it can still accurately measure the most damaging GDR. As a rule of thumb, we find that the standard deviation of the GDR should not exceed about one half of the transform-limited pulse duration, e.g. 240 fs for a 480 fs pulse. However, the performance is strongly dependent on the particular pattern of noise. On the other hand, using our measurement method to reconstruct the phase of the CFBG, we can simulate the compression performance by multiplying the CFBG complex spectrum with that of the stretched pulse. This provides a better predictor of individual device performance, while the standard deviation of GDR is more indicative of average device quality.

2. Measurement method: theory

While different GVD measurement methods have been proposed and demonstrated [8–10,12,13, 25,26], the most common GVD measurement method uses the differential phase shift between the two frequency sidebands of a modulated narrow-band tunable light source. Here, we rather use the fact that orthogonally polarized modes have the same temporal frequency, but different spatial frequencies. Measuring the differential phase of these two modes is achieved by first launching circularly polarized light, and measuring the reflection through an in-line polarizer [27,28]. A broadband optical source (BBS) passed through an in-line polarizer can be used, whose state of polarization can then be adjusted to circular with a polarization controller (PC). An optical spectrum analyzer (OSA) then measures the light reflected through the same polarizer. Since the phase matching condition for reflection from the CFBG actually involves the difference between the spatial (and not temporal) frequency of the light and that of the grating, each orthogonal mode will be reflected at a slightly different location along the CFBG, that satisfies their respective resonant Bragg condition. For a given chirp, wavelengths within the CFBG spectrum propagate further and further into it, so that the state of polarization at the polarizer will go through one spectral cycle for every additional beat length traveled along the CFBG and back. In a polarization-maintaining (PM) fiber, the typical beat length is about 2-3 mm, while the CFBG is typically 100 mm long. Therefore the reflected spectrum will show multiple cycles of high and low values, the phase of which is directly related to the group delay. This is but an intuitive description. We show below mathematically that the beat spectrum is directly related to the GVD, irrespective of the particular chirp function. For example, it can also measure the GVD of unchirped gratings.

The measurement setup is illustrated in Figure 1. The light from the broadband source travels to the CFBG through a 3 dB coupler, followed by a fiber polarizer (POL), and a polarization controller. The fiber used in that part is circular-core, non-PM fiber. The PM fiber pigtail of the CFBG under test is connected either with a fusion splice, or a mechanical splice. The reflection retrieved from the other branch of the coupler is sent to the optical spectrum analyzer (OSA). Alternatively, a tunable laser source could be used in conjunction with a photo-detector. Tunable lasers are usually already polarized, and in that case a second PC may be used before the polarizer to ensure maximum transmission through it.
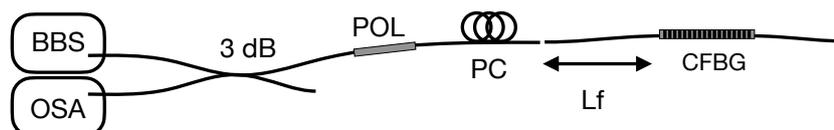

Figure 1. Measurement setup

For light at a given wavelength propagating to the CFBG and being reflected at one point along it, according to its chirp function, each orthogonally polarized mode will undergo a phase shift due to the length of the fiber pigtail to the CFBG, and from the group velocity dispersion of the CFBG itself. For the section of unbent, non-PM fiber between the PC and the PM fiber, the phase difference can be kept negligible because of the very low birefringence of the fiber, if care is taken to keep it straight and short (in our case less than 1m). If the two orthogonal modes of the PM fiber have effective indices n_+ and n_-, then the CFBG reflection spectra for each mode are shifted in frequency by an amount:

$$\delta\omega/\omega = (n_+ - n_-)/n_{av} = B, \tag{1}$$

where n_{av} is the average of n_+ and n_-, and B is the normalized birefringence. The total phase shift in each axis is then found to be:

$$\phi_\pm = \frac{2n_\pm L_f \omega}{c} + \phi_g(\omega \pm B\omega/2), \tag{2}$$

where $\phi_g(\omega)$ is the phase of the light reflected by the CFBG,. The phase difference $\Phi(\omega)$ between the two reflected modes is then:

$$\Phi(\omega) = \phi_+ - \phi_- = 2t_f B_f \omega + \phi'_g(\omega) B_g \omega, \tag{3}$$

where $t_f = n_{av}L_f/c$, and L_f is the length of the PM fiber pigtail from the connector to the CFBG. The first term on the right is the group delay of the fiber pigtail, while the second term is the group delay due to the CFBG. In Eq. (3) , we have purposefully distinguished between the birefringence in the fiber pigtail B_f and that within the CFBG B_g, to account for the possibility that the two could be different due to the photo-induced birefringence of the writing process. For a flat top 20 nm bandwidth CFBG, and a typical wavelength shift of about 0.25 nm (for $B = 2.5 \times 10^{-4}$) between the reflection spectra of the two polarized modes, the reflectivity is approximately the same for both polarizations, and the light reflected through the polarizer is given by:

$$R/R_{max} = \cos^2(\Phi(\omega)/2). \tag{4}$$

Given that the beat length of a typical PM fiber is of the order of 1-3 mm, and CFBGs can have lengths of 50-150mm, the reflection spectrum comprises a large number of cycles. The PM fiber pigtail having a typical length of about one meter also gives rise to multiple polarization rotations. Therefore,

it is difficult to know the absolute value of the phase with precision. However, each cycle corresponds to an additional 2π phase shift, so the curve of $\Phi(\omega)$ can be reconstructed from the beat pattern, albeit without a precise knowledge of the absolute value of the phase to within some multiple of 2π. On the other hand, the phase difference $\Delta\Phi$ between two adjacent frequencies separated by $\Delta\omega$ can be expressed as:

$$\Delta\Phi = \left[2B_f t_f + B_g \phi_g'(\omega) + B_g \omega \phi_g''(\omega)\right] \Delta\omega. \tag{5}$$

The first derivative $\phi_g'(\omega)$ is the group delay at frequency ω. The second derivative $\phi_g''(\omega)$ is the group velocity dispersion (GVD). The first frequency point on the edge of the spectrum ω_0 (for example corresponding to 3 dB below the peak reflection) can be defined as having a group delay of t_f, so that the group delay at that frequency $\phi_g'(\omega_0)$ is included in the total delay t_f from the polarizer up to that point. The following frequency point, at $\omega_1 = \omega_0 + \Delta\omega$ is then found to have :

$$\phi_g''(\omega_1) = \frac{1}{B_g \omega_1} \left[\Delta\Phi/\Delta\omega - 2B_f t_f - B_g \phi_g''(\omega_0)\Delta\omega\right], \tag{6}$$

where $\phi_g''(\omega_0)\Delta\omega$ is the additional group delay between ω_0 and ω_1. One can thus reconstruct $\phi_g''(\omega_n)$ recursively:

$$\phi_g''(\omega_n) = \frac{1}{B_g \omega_n} \left[\Delta\Phi/\Delta\omega - 2B_f t_f - B_g \sum_{i=0}^{n-1} \phi_g''(\omega_i)\Delta\omega\right]. \tag{7}$$

The value of the group delay at frequency ω_n is given by:

$$\phi_g'(\omega_n) = \sum_{i=0}^{n} \phi_g''(\omega_i)\Delta\omega. \tag{8}$$

This allows the value of B_g to be extracted from the reconstructed group delay curve, using knowledge of both the length L_g of the CFBG and its bandwidth W_g. For a value $t_g = n_{av}L_g/c$, and knowing the difference between the final phase and the initial phase $\Phi(\omega_f) - \Phi(\omega_0)$, we find:

$$B_g = \frac{\left(\Phi(\omega_f) - \Phi(\omega_0)\right) - 2t_f B_f W_g}{2\omega_f t_g}. \tag{9}$$

The difference between B_g and B_f thus represents the photo-induced birefringence from the grating writing process.

For a CFBG used as a pulse stretcher in a CPA laser system, the higher order values of the Taylor-series expansion of the phase of the reflected wave are important to know as they have to match those of the compressor at the output of the amplifier. The phase $\phi(\omega)$ is thus expanded as:

$$\phi(\omega) = \phi(\omega_c) + D_1(\omega_c)\delta\omega + \frac{D_2(\omega_c)}{2}\delta\omega^2 + ... + \frac{D_n(\omega_c)}{n!}\delta\omega^n, \tag{10}$$

where $D_n = \partial^n \phi/\partial\omega^n$, and $\delta\omega = (\omega - \omega_c)$. If the curve $\phi_g'(\omega)$ is fitted around a central frequency ω_c with a polynomial of order n, such that $\phi_g' = a_0 + a_1(\omega - \omega_c) + ... + a_n(\omega - \omega_c)^n$, then we find:

$$D_n = (n-1)!a_{n-1}. \tag{11}$$

The resolution of the measurement is limited both by the OSA resolution (20 pm for modern instruments), but mostly by the beat length of the fiber, corresponding to a wavelength shift of 0.25 nm for $B = 2.5 \times 10^{-4}$. We show through simulations in the next section that the most deleterious GDR have spectral periods of the order of the pulse bandwidth, and are readily captured by our method, despite this resolution limitation.

3. Simulations and performance analysis

We first estimate the performance of the measurement method by comparing the GVD values and GDR obtained from the direct numerical computation of the CFBG spectrum with various amounts of noise, with those obtained from a simulated measurement using the computed amplitude and phase of the reflection spectrum, and taking into account the fiber birefringence and resolution of the OSA. The phase of the CFBG extracted from both the direct computation and the simulated measurement is also used to compare the pulse compression performance with an optimized grating pair compressor. For the rest of the paper, the value of GDR is taken as the standard deviation of the group delay over a given spectral bandwidth, and is expressed in fs, while the noise in the grating period is expressed as the standard deviation of the period over the CFBG length, measured in pm.

CFBGs of 92 mm length, with a super-Gaussian spatial profile (exponent of 28) having a FWHM of 83 mm, and linear and quadratic chirp values of -0.1935 nm/mm, and -0.00026 nm/mm^2 respectively, were simulated with the well-known matrix method. A linear taper of the grating strength of 13% across its length was added to obtain a flat reflection and transmission spectrum, as otherwise the quadratic chirp results in a slanted spectrum. The quadratic chirp is required to match the higher order dispersion of a grating-pair compressor. The coupling constant was adjusted to give 50% reflectivity, a typical value for practical devices, limited by the amount of coupling by the CFBG into the fiber cladding modes. The wavelength step was typically 2 pm or less, and spatial step 0.05 mm or less. Noise could be introduced to either the period or the amplitude with a filtered white noise generator, to generate GDR patterns similar to those of our actual measurements. Alternatively, we also introduced periodic oscillations with a single spatial frequency.

The measurement was simulated by taking the numerically computed spectrum, shifting the frequency by plus or minus the amount of Eq. (1), summing the two resulting complex spectral amplitudes, taking the square modulus of their sum and dividing by the average of the squared moduli of the two (equivalent to the measurement normalization using the reflection trace). The resulting beat spectrum is then filtered to simulate the OSA instrumental resolution of 20 pm. The algorithm to extract the phase from the beat spectrum is the same as used to process the actual measurement data.

The various orders of GVD are obtained by fitting the phase to a high-order polynomial. The group delay itself is obtained from Eq. (8). Generally, only the first three orders, that is D_2 to D_4, are relevant, and higher order fits do not significantly change their values. GDR are calculated by subtracting the 3rd order polynomial fit of the group delay from the computed (and eventually the measured) exact group delay.

Pulse recompression is then simulated by summing the phase of the CFBG to that of a grating pair compressor (calculated to all orders), using both the computed phase, or that retrieved from the simulated measurement algorithm. The amplitude is the square root of the reflection spectrum. The laser spectrum used is based on a typical Yb-based femtosecond laser, with a bandwidth of 2.3 nm, and a sech^2 shape.

The CFBG can have fluctuations in both its amplitude and period. Both result in GDR as well as in a noisy transmission spectrum (Figure 3). Amplitude fluctuations also give rise to period fluctuations, if the average refractive index fluctuates (e.g. due to laser power fluctuations during the writing process). Pure amplitude fluctuations give rise to noise in the transmission spectrum, but produce insignificant GDR, therefore period fluctuations are the most important. Since both result in a noisy transmission spectrum, the latter cannot distinguish between the two, and is not a good indicator of device performance. Only the GDR can predict the device performance, so we focus on those.

First of all, for a perfect grating with the above design, a comparison between the values of D_2 to D_4 obtained by direct computation, and by simulated measurement, were the same to within less than 1%. In such case, there are no GDR, although the standard deviation is not zero due to a slow and small fluctuation from the ideal group delay. Recompression of a 482 fs pulse (transform-limited from the 2.3 nm laser spectrum), after stretching with the CFBG, yields a 493 fs pulse by optimizing the compressor

6 of 12

angle and grating separation. The 11 fs penalty is due to the mismatch in D_4 , as we consider a CFBG made with a phase mask with only up to a quadratic chirp (corresponding to the devices we measured). The CFBG has a D_4 twice that of the compressor, resulting in a slightly broadened pulse. On the other hand, the pulse has a high quality fit to a sech^2 shape with no sidebands. To compute the Strehl ratio in the presence of noise, we use this slightly longer pulse as reference, giving a ratio of 1.00 for this ideal case. The Strehl ratio for other cases is then computed from the ratio of the peak power to the integrated pulse energy, using the computed ratio of this ideal case as a normalizing factor.

To assess the resolution of the measurement, and its ability to capture the most deleterious GDR, we first introduce a single spatial frequency ripple with 10 pm amplitude to the ideal chirp function, with periods from 0.5 mm to 30 mm. This results in periodic oscillations in the reflection/transmission spectrum, as well as in the group delay. The GDR is calculated across the 3 dB bandwidth of the spectrum, as well as the recompressed pulse width and Strehl ratio for both the directly computed and simulated measurement cases. As seen in Figure 2, the ratio between the GDR of the simulated measurement and directly computed cases increases to unity as the spatial period increases, reaching 90% for a period of 6 mm, slightly more than two beat lengths. For small periods, the amplitude of the group delay oscillations can be very large, and show a kind of periodic fluctuation with the period, which disappears for periods larger than about 3mm. We could not explain the origins of those fluctuations. On the other hand, although they can have amplitudes of 1000 fs peak to peak, they have little effect on the pulse duration and quality below that 6 mm threshold, and the Strehl ratio remains above 0.99. As the period increases, the group delay modulation creates satellite pulses that get stronger and closer to the central peak, as already discussed in ref. [11]. Therefore, it appears that even though the beat length limits the spectral resolution of the measurement, the latter remains high enough to capture the most deleterious regime of GDR. It should also be noted that most effects responsible for fluctuations in the grating period occur on scales longer than that of the laser beam used to write the grating (with the usual scanning beam technique), which is about 1 mm.
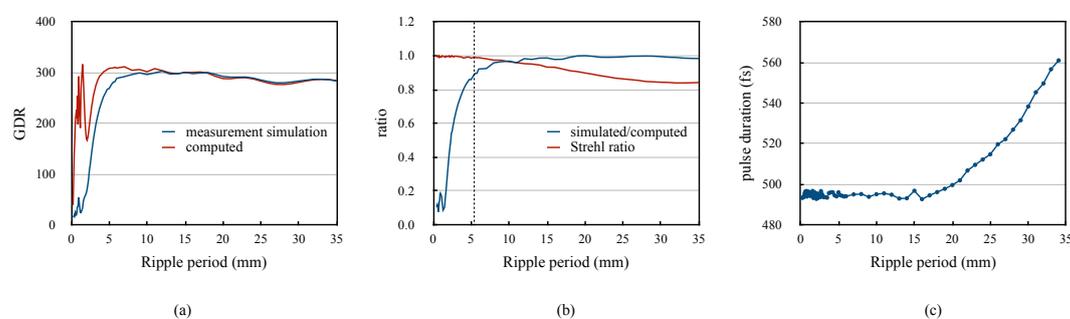

Figure 2. (a) GDR vs ripple period for the computed and simulated measurement cases ; (b) Ratio of GDR for simulated measurement to computed, and Strehl ratio; (c) Pulse duration vs Ripple period

Next we introduce random noise patterns, using white noise and a low pass filter to more or less emulate the GDR patterns obtained from actual measurements. For standard deviations of period fluctuations ranging from 0 to 15 pm, we simulated over 100 CFBGs. The noise creates both fluctuations in the transmission spectrum and the group delay response, and affects the pulse duration and Strehl ratio. Figure 3 shows three examples with 0, 7.9, and 16.4 pm noise. GDR and recompressed pulses are shown for both the directly computed and simulated measurement cases, but they are virtually identical. Figure 4(a) shows that the GDR is linearly related to the period noise. However, the net effect of the GDR depends on the particular noise pattern. Figure 4(b) and (c) shows the pulse duration and Strehl ratio as a function of GDR for all the gratings simulated. It can be seen that the proportion of "good" pulses decreases rapidly over a certain value of noise, although in many cases the pulse is still "good enough", depending on the particular acceptable performance target. In the case of the

particular CFBG design studied here, a threshold of about 230 fs is estimated above which the yield of good devices becomes too low, as indicated by the shadowed areas in Figure 4. This is about one half of the ideal pulse duration. However, in many cases CFBGs with higher GDR are still acceptable. Therefore, while the GDR is a good indicator of average device quality, individual device measurement and simulation of pulse recompression is a better predictor of performance.
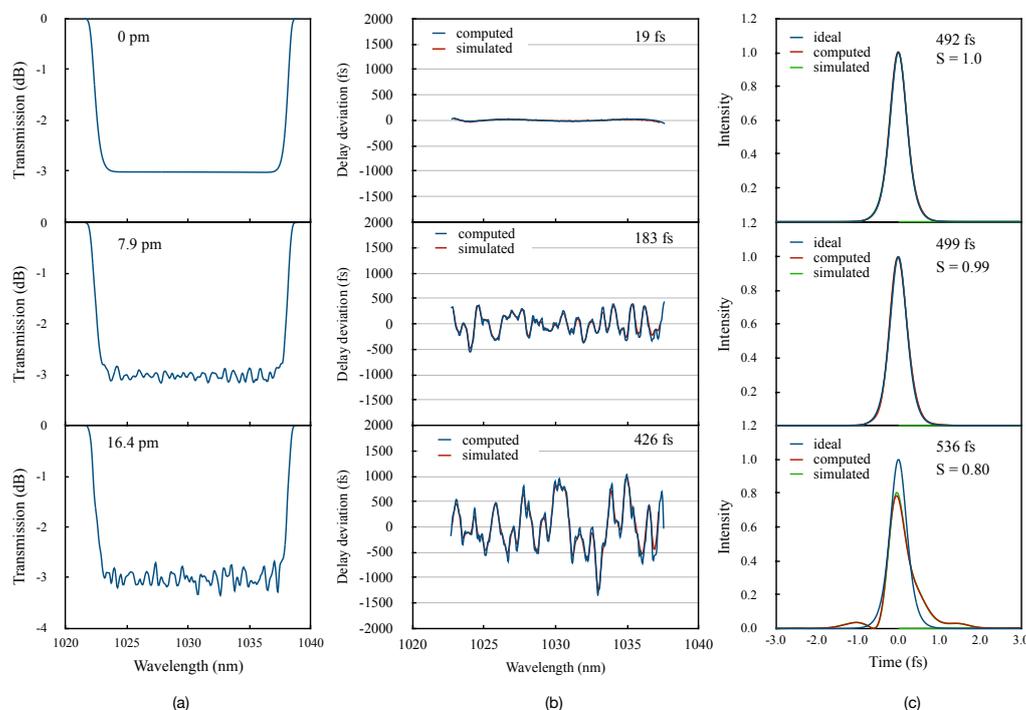
Figure 3. (a) Transmission spectrum; (b) group delay ripples; (c) simulated compressed pulse for CFBGs with 0, 7.9 pm, and 16.4 pm period fluctuations.
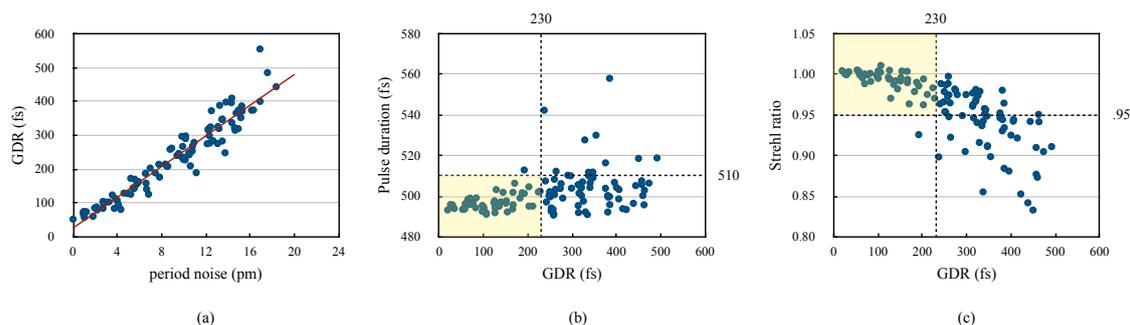
Figure 4. (a) GDR vs period noise ; (b) Pulse duration vs period noise; (c) Strehl ratio vs period noise

In any case, to accurately measure such small amount of GDR, the actual measurement should have a resolution much below that threshold, which we demonstrate experimentally in the next section.

4. Measurement

The measurement procedure is the following. The beat spectrum is obtained by first taking the reflection spectrum of the CFBG without the polarizer (POL) and polarization controller (PC), and storing it as a reference trace. Since the BBS is unpolarized, this is an average of the reflection spectra for both polarization axis. The OSA trace is then set as the difference between the measured trace

and the reference trace (on a logarithmic scale). Then the POL and PC are added to the circuit, which results in spectral oscillations (the beat spectrum), and the PC is adjusted for maximum contrast of the beat spectrum (typically more than 10 dB). An example of beat spectrum is shown in Figure5(b), consisting of 57 peaks over a bandwidth of 15.4 nm.

To process the data, we implemented a phase reconstruction algorithm that takes into account the limited contrast of the beat spectrum caused by the finite resolution of the OSA (20 pm). The group delay is then obtained using the algorithm of Eq. (7). Fitting the group delay with a third order polynomial, and subtracting the raw curve readily gives the GDR, as in the simulations above. The phase of the CFBG is obtained by integrating the reconstructed group delay (which includes the GDR). Together with the reflection spectrum, it is used to simulate the stretching/compression of a pulse, using the typical spectrum of our femtosecond laser (2.3 nm bandwidth, sech^2 shape). The compressor grating angle, and grating separation are then optimized to give the shortest pulse with the highest Strehl ratio.

Figure 5 shows the reflection, transmission, beat spectrum and group delay of an actual CFBG with a total length of 92 mm, and 1 dB bandwidth of 15.4 nm, written in a Coherent PM980 fiber. The spectra were taken with a Yokogawa AQ6370D optical spectrum analyzer using the maximum resolution of 20 pm, thus giving over 10,000 data points over the entire bandwidth. The transmission spectrum shows a typical slant, introduced to compensate for the loss of light to cladding modes at shorter wavelengths, so that the reflection spectrum itself viewed from the long wavelength side is nearly flat.

The calculation of the group delay requires a knowledge of the fiber birefringence. As it can change from one fiber batch to another, it is better to measure it, if not for every device, at least for batches made with the same fiber spool. In order to obtain the value of B_f, the spectrum of the light reflected from the cleaved far end of the CFBG pigtail was measured over a range of wavelengths outside of the CFBG bandwidth (from 1045 nm to 1065 nm). That spectrum also shows oscillations due to the $t_f\omega$ term in Eq.(3), and the birefringence can be obtained by measuring the frequency difference between two peaks, that correspond to an integer value of 2π. We then get:

$$B_f = \frac{2N\pi}{t_p\Delta\omega},\tag{12}$$

where $t_p = 2n_{av}L_p/c$ is the round trip delay of the total pigtail of length L_p. In practice, to obtain an even more accurate value, we used the same phase retrieval method as used for the beat spectrum, and performed a quadratic fit, extrapolated to the device center wavelength. We found that $B_f = 2.5 \times 10^{-4}$ for the particular device measured (Coherent PM980 fiber).
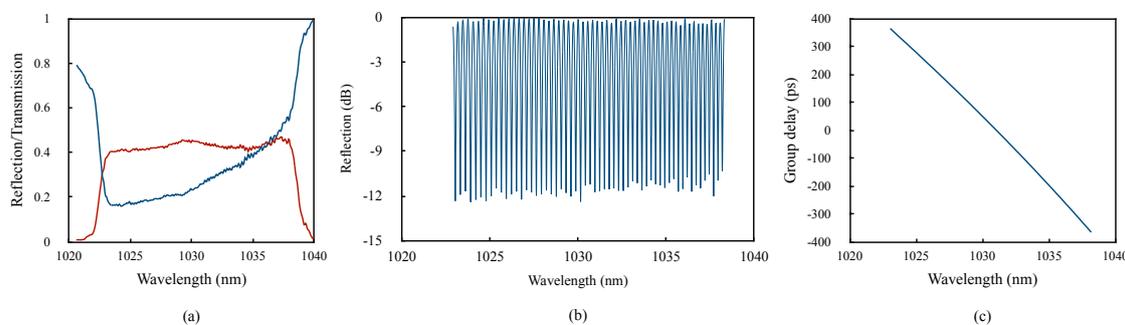

Figure 5. (a) Reflection and transmission; (b) Beat spectrum; (c) Reconstructed group delay

The measured values of D_2, D_3 and D_4 are respectively 27.9 ps^2, -0.263 ps^3, and 0.0064 ps^4. To obtain the value of B_g, a knowledge of the length and bandwidth of the CFBG is required. The effective length over given bandwidth limits (e.g. -1 dB), is obtained from simulation of the grating response,

knowing the design of the phase mask used to fabricate it (linear and quadratic chirp). Using this value, the difference between B_g and B_f was found to be about 1×10^{-5}, which is not unexpected for photo-induced birefringence [29–33]. This difference in B was systematic for all CFBGs tested made in the same fiber, and different for CFBGs made in a different fiber (also with a different sign in one case). Such a difference does not appear in simulated gratings, where we assume $B_g = B_f$ and therefore cannot be attributed to any imprecision of the data processing algorithm itself. We conclude that it probably truly reflects the photoinduced birefringence from the grating writing process.

Figure 6 shows the GDR, obtained by subtracting a third order polynomial fit of the group delay from the reconstructed curve. The standard deviation in this case is 161 fs. The transmission spectrum itself shows only small ripples, readily indicating a good device quality. Two consecutive measurements are shown, as well as the difference between the two measurements. Spectral features narrower than 0.1 nm and ripples less than 50 fs are clearly and reproducibly resolved. The difference between the two measurements does not exceed 100 fs (except for a very narrow spike), and its standard deviation is 29 fs. It must be noted, however, that good care must be taken not to disturb the fiber in any way during the measurement process. Any bend or pressure on the fiber leading to the CFBG, which introduces coupling between the orthogonally polarized modes, is likely to result in an erroneous measurement. Narrow spikes in the reflection spectrum can also introduce some error, since the spectrum is assumed to be flat, but those are also indicative of a defective device anyway. Although an accurate estimation of resolution would require more extensive statistical measurements, it appears to be at least as good as 50 fs, as features that small are clearly resolved. This is on par with much more expensive commercial instruments.
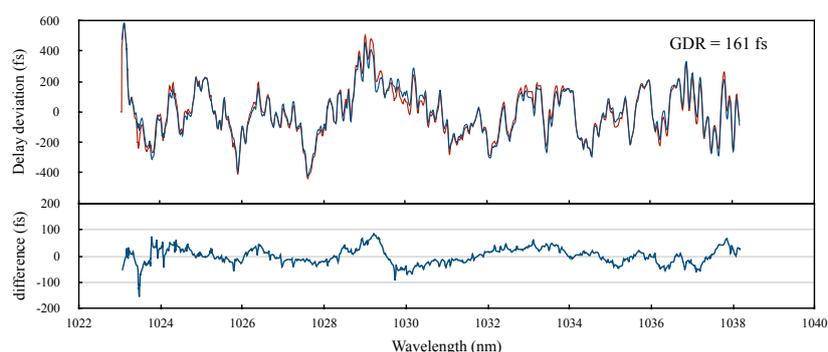
Figure 6. Transmission spectrum, group delay ripples, and simulated compressed pulse for CFBGs with 0, 3.85 mrad, and 8.5 mrad rms phase noise

The simultated recompressed pulse duration for the device of Figure 5 is predicted to be 499 fs. The actual recompressed pulse using an optimized grating pair has a autocorrelation width of 700 fs, giving a 500 fs sech^2 pulse, in agreement with the prediction.

5. Discussion and Conclusion

We have presented a simple measurement method of the group delay and group delay ripples of CFBG used as stretchers in CPA laser system, together with an analysis of the degradation of the performance due to noise in their chirp profile. The great advantage of our method is that a quick and complete characterization of the CFBG, including reflection, transmission, and dispersion, can be done at the same time with a simple measurement setup. Apart from a polarizer and polarization-controller, no additional equipment is required. Furthermore, a reconstruction of the phase of the CFBG allows a simulation of the pulse recompression for each individual device.

Our analysis shows that fluctuations of the period of the CFBG are the main source of group delay ripples, and that ripples with spectral periods of the order of the laser bandwidth are the most deleterious. The spectral resolution of the GDR using our measurement method is limited by the beat

length of the PM fiber, but is more than enough to capture those longer period GDR. We found that the recompressed pulse duration and quality degrade for GDR larger than about one half of the pulse duration. For sub-ps pulses, this means that a GDR resolution much better than the pulse duration is required. Our measurements show that we can attain resolution better than 50 fs.

Although the results presented here were obtained with a CFBG written in a PM fiber, the method can also be used in a non-PM fiber, as was shown in [28]. In such case, the value of B is much smaller, typically less than 10^{-6}, and the entire spectrum of the CFBG will typically only show a fraction of one cycle. In [28], the polarization was adjusted so that the reflection was at a minimum at the short wavelength edge of the CFBG spectrum. The value of the normalized reflection could then readily give an accurate value of the phase over the entire spectrum. In such case, the measurement is no longer limited by the fiber birefringence, but by the instrument spectral resolution.

In conclusion, the proposed method has been demonstrated to provide a quick, simple and accurate measurement of the GVD parameters of CFBGs written in PM fiber, and the level of group delay ripple, useful to assess their performance as pulse-stretchers in CPA laser systems.

Abbreviations

The following abbreviations are used in this manuscript:

BBS	Broad Band Source
BER	Bit Error Rate
CFBG	Chirped Fiber Bragg Grating
CPA	Chirped Pulse Amplification
GDR	Group Delay Ripple
GVD	Group Velocity Dispersion
OSA	Optical Spectrum Analyzer
PC	Polarization Controller
PM	Polarization Maintaining

References

1. Ouellette, F. Dispersion cancellation using linearly chirped Bragg grating filters in optical waveguides. *Opt. Lett.* **1987**, *12*, 847–849. doi:10.1364/OL.12.000847.
2. Ouellette, F.; Krug, P.; Stephens, T.; Dhosi, G.; Eggleton, B. Broadband and WDM dispersion compensation using chirped sampled fibre Bragg gratings. *Electronics Letters* **1995**, *31*, 899–901(2).
3. Galvanauskas, A.; Fermann, M.E.; Harter, D.; Sugden, K.; Bennion, I. All fiber femtosecond pulse amplification circuit using chirped Bragg gratings. *Applied Physics Letters* **1995**, *66*, 1053–1055, [https://doi.org/10.1063/1.113571]. doi:10.1063/1.113571.
4. Imeshev, G.; Hartl, I.; Fermann, M.E. Chirped pulse amplification with a nonlinearly chirped fiber Bragg grating matched to the Treacy compressor. *Opt. Lett.* **2004**, *29*, 679–681. doi:10.1364/OL.29.000679.
5. Želudevičius, J.; Danilevičius, R.; Regelskis, K. Optimization of pulse compression in a fiber chirped pulse amplification system by adjusting dispersion parameters of a temperature-tuned chirped fiber Bragg grating stretcher. *J. Opt. Soc. Am. B* **2015**, *32*, 812–817. doi:10.1364/JOSAB.32.000812.
6. Wang, M.X.; Li, P.X.; Xu, Y.T.; Zhu, Y.C.; Li, S.; Yao, C.F. An All-Fiberized Chirped Pulse Amplification System Based on Chirped Fiber Bragg Grating Stretcher and Compressor. *Chinese Physics Letters* **2022**, *39*, 024201. doi:10.1088/0256-307X/39/2/024201.

7.   Lampen, J.; Tani, F.; Li, P.; Lee, K.F.; Jiang, J.; J.Russell, P.S.; Fermann, M.E. Compact Yb fiber few-cycle pulse source based on precision pulse compression and shaping with an adaptive fiber Bragg grating. *Opt. Express* **2023**, *31*, 8393–8399. doi:10.1364/OE.483277.

8.   Lauzon, J.; Thibault, S.; Martin, J.; Ouellette, F. Implementation and characterization of fiber Bragg gratings linearly chirped by a temperature gradient. *Opt. Lett.* **1994**, *19*, 2027–2029. doi:10.1364/OL.19.002027.

9.   Dyer, S.D.; Rochford, K.B.; Rose, A.H. Fast and accurate low-coherence interferometric measurements of fiber Bragg grating dispersion and reflectance. *Opt. Express* **1999**, *5*, 262–266. doi:10.1364/OE.5.000262.

10.   Fortenberry, R.; Sorin, W.; Hernday, P. Improvement of group delay measurement accuracy using a two-frequency modulation phase-shift method. *IEEE Photonics Technology Letters* **2003**, *15*, 736–738. doi:10.1109/LPT.2003.810251.

11.   Littler, I.C.M.; Fu, L.; Eggleton, B.J. Effect of group delay ripple on picosecond pulse compression schemes. *Appl. Opt.* **2005**, *44*, 4702–4711. doi:10.1364/AO.44.004702.

12.   Ahn, T.J.; Park, Y.; na, J.A. Fast and accurate group delay ripple measurement technique for ultralong chirped fiber Bragg gratings. *Opt. Lett.* **2007**, *32*, 2674–2676. doi:10.1364/OL.32.002674.

13.   Santos, M.C.; De Bernardo-Rodi, S.P.; Mitre-Gutierrez, M.A. New Modulation Zero-Shift Method to Characterize Fast Group Delay Ripple of Dispersion-Compensating Fiber Bragg Gratings. *IEEE Photonics Technology Letters* **2007**, *19*, 1298–1300. doi:10.1109/LPT.2007.902296.

14.   Ouellette, F. The Effect of Profile Noise on the Spectral Response of Fiber Gratings. Bragg Gratings, Photosensitivity, and Poling in Glass Fibers and Waveguides: Applications and Fundamentals. Optica Publishing Group, 1997, p. BMG.13. doi:10.1364/BGPPF.1997.BMG.13.

15.   Ennser, K.; Ibsen, M.; Durkin, M.; Zervas, M.; Laming, R. Influence of nonideal chirped fiber grating characteristics on dispersion cancellation. *IEEE Photonics Technology Letters* **1998**, *10*, 1476–1478. doi:10.1109/68.720299.

16.   Feced, R.; Zervas, M. Effects of random phase and amplitude errors in optical fiber Bragg gratings. *Journal of Lightwave Technology* **2000**, *18*, 90–101. doi:10.1109/50.818912.

17.   Jamal, S.; Cartledge, J.C. Variation in the Performance of Multispan 10-Gb/s Systems Due to the Group Delay Ripple of Dispersion Compensating Fiber Bragg Gratings. *J. Lightwave Technol.* **2002**, *20*, 28.

18.   Niemi, T.; Uusimaa, M.; Ludvigsen, H. Limitations of phase-shift method in measuring dense group delay ripple of fiber Bragg gratings. *IEEE Photonics Technology Letters* **2001**, *13*, 1334–1336. doi:10.1109/68.969899.

19.   Sumetsky, M.; Eggleton, B.J.; de Sterke, C.M. Theory of group delay ripple generated by chirped fiber gratings. *Opt. Express* **2002**, *10*, 332–340. doi:10.1364/OE.10.000332.

20.   Lachance, R.L.; Morin, M.; Painchaud, Y. Group delay ripple in fibre Bragg grating tunable dispersion compensators. *Electronics Letters* **2002**, *38*, 1.

21.   Yan, L.S.; Luo, T.; Yu, Q.; Xie, Y.; Feng, K.M.; Khosravani, R.; Willner, A. Investigation of performance variations due to the amplitude of group-delay ripple in chirped fiber Bragg gratings. *Optical Fiber Technology* **2006**, *12*, 238–242. doi:https://doi.org/10.1016/j.yofte.2006.01.001.

22.   Litchinitser, N.; Li, Y.; Sumetsky, M.; Westbrook, P.; Eggleton, B. Tunable Dispersion Compensation Devices: Group Delay Ripple and System Performance. Optical Fiber Communication Conference. Optica Publishing Group, 2003, p. TuD2.

23.   Eiselt, M.; Clausen, C.; Tkach, R. Performance characterization of components with group delay fluctuations. *IEEE Photonics Technology Letters* **2003**, *15*, 1076–1078. doi:10.1109/LPT.2003.815356.

24.   Komukai, T.; Inui, T.; Nakazawa, M. Origin of group delay ripple in chirped fiber Bragg gratings and its effective reduction method. *Electronics and Communications in Japan (Part II: Electronics)* **2003**, *86*, 76–84, [https://onlinelibrary.wiley.com/doi/pdf/10.1002/ecjb.10007]. doi:https://doi.org/10.1002/ecjb.10007.

25.   Ryu, S.; Horiuchi, Y.; Mochizuki, K. Novel chromatic dispersion measurement method over continuous Gigahertz tuning range. *Journal of Lightwave Technology* **1989**, *7*, 1177–1180. doi:10.1109/50.32379.

26.   Gifford, D.K.; Soller, B.J.; Wolfe, M.S.; Froggatt, M.E. Optical vector network analyzer for single-scan measurements of loss, group delay, and polarization mode dispersion. *Appl. Opt.* **2005**, *44*, 7282–7286. doi:10.1364/AO.44.007282.

27.   Ouellette, F.; Yao, F.; Wang, J.; Li, J. A Simple Method to Measure the Group Delay of Chirped Fiber Gratings in Polarization-Maintaining Fiber. Optica Advanced Photonics Congress 2022. Optica Publishing Group, 2022, p. BTh3A.3. doi:10.1364/BGPPM.2022.BTh3A.3.

28. Ouellette, F.; Stepanov, D. A new technique for measuring the group delay of chirped fiber Bragg gratings. Proceedings of Optical Fiber Communication Conference (, 1997, pp. 153–154. doi:10.1109/OFC.1997.719775.

29. Ouellette, F.; Gagnon, D.; Poirier, M. Permanent photoinduced birefringence in a Ge doped fiber. *Applied Physics Letters* **1991**, *58*, 1813–1815, [https://doi.org/10.1063/1.105097]. doi:10.1063/1.105097.

30. Meyer, T.; Nicati, P.A.; Robert, P.A.; Varelas, D.; Limberger, H.G.; Salathé, R. Birefringence writing and erasing in ultra-low-birefringence fibers by polarized ultraviolet side-exposure: origin and applications. *Optical Review* **1997**, *4*, A53. doi:10.1007/BF02935990.

31. Canning, J.; Deyerl, H.J.; Sørensen, H.R.; Kristensen, M. Ultraviolet-induced birefringence in hydrogen-loaded optical fiber. *Journal of Applied Physics* **2005**, *97*, 053104, [https://doi.org/10.1063/1.1856215]. doi:10.1063/1.1856215.

32. Jiang, L.; Zhang, D.; Li, L.; Yuan, S.; Dong, X.; others. A Novel Method for Measuring Photo-Induced Birefringence of Photosensitive Fibers. *Acta Optica Sinica* **2003**, *23*, 53–54.

33. Lu, P.; Mihailov, S.J.; Grobnic, D.; Walker, R.B. Comparison of the Induced Birefringence in Fiber Bragg Gratings Fabricated with Ultrafast-IR and CW-UV Lasers. 2006 European Conference on Optical Communications, 2006, pp. 1–2. doi:10.1109/ECOC.2006.4801001.